Evidence of Rayleigh-Hertz Surface Waves and Shear Stiffness Anomaly in Granular Media

L. Bonneau, B. Andreotti, and E. Clément

PMMH, ESPCI, CNRS (UMR 7636) and Universités Paris 6 & Paris 7, 10 rue Vauquelin, 75005 Paris, France

(Received 11 March 2008; published 9 September 2008)

Using the nonlinear dependence of sound propagation speed with pressure, we evidence the anomalous elastic softness of a granular packing in the vicinity of the jamming transition. Under gravity and close to a free surface, the acoustic propagation is only possible through surface modes guided by the stiffness gradient. These Rayleigh-Hertz modes are evidenced in a controlled laboratory experiment. The shape and the dispersion relation of both transverse and sagittal modes are compared to the prediction of nonlinear elasticity including finite size effects. These results allow one to access the elastic properties of the packing under vanishing confining pressure.

DOI: 10.1103/PhysRevLett.101.118001 PACS numbers: 45.70.Ht, 05.45.Xt, 43.75.+a, 91.60.Lj

The evidence of anomalous mechanical properties in static, disordered granular assemblies of frictionless spheres has brought a new perspective on glassy systems [1]. In such a noncohesive material, the external pressure is the only source of confinement that may jam the packing in the rigid phase. Thus, at zero thermal agitation, a solid-fluid transition would be reached under a vanishing confining pressure, i.e., when the packing becomes a marginal solid with just the minimal amount of contacts per grain Z suited to sustain a large scale elastic network, i.e., at isostaticity ($Z = Z_{\mathrm{iso}}$). Near jamming, this model system presents excess low frequency modes, called "soft modes," whose spatial extension diverges at the critical point [2] and which cause a nonaffine linear response. It has been shown numerically and theoretically that these weak floppy modes make the ratio G/K of shear modulus to bulk modulus vanish at the jamming transition [2]. This is similar to the behavior of many other disordered condensed systems—mostly multistable systems such as regular fluids trapped in a glassy phase [3]—that also lose their shear rigidity (characteristic of ordinary solids) when they are on the verge of yielding. Can this anomalous linear response be evidenced experimentally? Is this simplified jamming scenario robust enough to describe real granular matter that includes frictional contacts [4,5], gravity loading, or nonspherical particles? These are fundamental questions when one seeks to establish a generic picture for the glassy transition of weak solids viewed from the jammed phase.

In this Letter, we show that the propagation of surface sound waves provides insights into the structure of the elastic networks in the vicinity of jamming. This experimental technique allows one to measure the elastic properties of a granular packing under vanishing pressure, i.e., close to a free surface and under gravity loading. In ordinary elastic solids, surface waves (called Rayleigh waves) are a combination of compression and shear waves, and they travel at a speed slightly smaller than bulk shear waves (~ 5000 m/s for glass). Acoustic measurements in granular matter with a free surface have been performed in the context of ethology [6]—numerous species living at the desert surface use sound waves to probe their environment—and seismic geology [7,8]. In both cases, a surprisingly low speed of sound (~ 50 m/s) was observed. However, it is only recently that two independent theoretical calculations based on slightly different models of nonlinear elasticity [9,10] have shown that these surface waves should be ascribed to a gravity induced index gradient, which plays the role of a waveguide and allows for the propagation of an infinite collection of surface modes.

To clarify the theoretical issues addressed here, let us rephrase in the framework of nonlinear elasticity the predictions of Wyart *et al.* [2] on the elastic anomaly induced by soft modes. For geometrical reasons, the Hertz contact force between two grains depends nonlinearly on their relative interpenetration. On this basis, the macroscopic elastic free energy of an isotropic granular packing can be written in a general form [11]:

$$\mathcal{F} = E\left(\tfrac{2}{5}\mathcal{B}\delta^{5/2} + \mathcal{A}\,\delta^{1/2}u^0_{ij}u^0_{ij}\right), \qquad (1)$$

where u_{ij} is the coarse-grained strain tensor, $\delta = -\mathrm{Tr}(u_{ij})$ is the volumic compression, and $u^0_{ij} = u_{ij} + \frac{\delta}{3}\delta_{ij}$ is the traceless strain tensor. $\mathcal{A}$ and $\mathcal{B}$ are two dimensionless elastic coefficients that characterize the material stiffness under shear and compression, respectively. We assume that the average number of contacts per grain Z is sufficient to characterize the microscopic packing geometry and thus that $\mathcal{A}$ and $\mathcal{B}$ are functions of Z. Indeed, in a frictional packing, different values of Z can be obtained under the same pressure p; Z and p are thus independent state variables [5]. It should be emphasized that $\mathcal{F}$ is not supposed to describe the stress-strain curve obtained from a loading test, which is composed by a series of elastic loadings at fixed Z and of plastic events during which Z changes.

Assuming homogeneity and identifying macroscopic and microscopic strains, mean-field theory (see [12] and references therein) predicts that $\mathcal{A}$ and $\mathcal{B}$ vary linearly in $\mathcal{Z}$ and thus remain finite when $p \to 0$ [10]. However, jamming theory [2] predicts that upon approaching isostaticity, the shear modulus G presents a critical behavior, $G = \mathcal{A}E^{2/3}(P/\mathcal{B})^{1/3} \sim (\mathcal{Z} - \mathcal{Z}_{\rm iso})P^{1/3}$, coming through its coupling with the excess of contacts above the isostatic value, which itself scales as $\mathcal{Z} - \mathcal{Z}_{\rm iso} \sim P^{1/3}$. Then, the ratio of shear to bulk modulus $K = (\mathcal{B}E)^{2/3}P^{1/3}$ should vanish with pressure as $G/K = \mathcal{A}/\mathcal{B} \sim P^{1/3}$. In Ref. [10], the surface elastic modes were derived for the free energy (1). The guided waves propagate through an infinite though discrete collection of modes polarized sagittally (i.e., a compound of vertical and longitudinal displacements vibrating in quadrature) or transversely. The mode labeled n of wavelength λ penetrates the sample over a typical depth $n\lambda$ and thus feels a typical pressure $p = \rho g n \lambda$. Consequently, the mean-field theory predicts a velocity dependence of the form $v \sim (n\lambda)^{1/6}$. Alternatively, for low frequency modes where elastic coupling with shear stiffness is dominant, the soft-modes theory would predict $v \sim (n\lambda)^{1/3}$. Consequently, the dispersion relation of surface waves constitutes a direct experimental test for the existence of a shear stiffness anomalous scaling. Let us emphasize again that the reality of the jamming point as a critical point was assessed for frictionless soft spheres, but there are several indications that this line of ideas could be generalized to frictional packing [4,13] and even to glasses [14].

As confirmed by preliminary experiments [15], the weak dependence of the speed of sound on n makes the experiment very difficult to control and almost impossible to analyze. Indeed, using any standard source, a huge number of propagating modes are excited that remain superimposed over large distances. To bypass this problem, we have successfully designed an experiment that isolates the first sagittal and transverse modes. For this, measurements are performed in a rectangular channel of width $W = 20$ cm and length 180 cm, which serves as a second waveguide [Fig. 1(a)]: the lateral boundary conditions impose a relation between the measured wavelength λ and the wavelength λ_∞ that would be selected in an infinitely large channel, at the same frequency:

$$\lambda_\infty = \left[\frac{1}{\lambda^2} + \left(\frac{m}{2W}\right)^2\right]^{-1/2}, \qquad (2)$$

where m is the transverse mode number ($m = 1$ here). Moreover, the sources are conceived and tuned to excite essentially the modes $n = 1$: sagittal waves are produced by an electromagnetic shaker (without any spring) whose axis is finely guided by a ball bearing slider coupled to a very rigid transverse metallic blade; transverse waves are produced by a rough cylinder inside which a permanent magnet vibrates under the action of a magnetic field

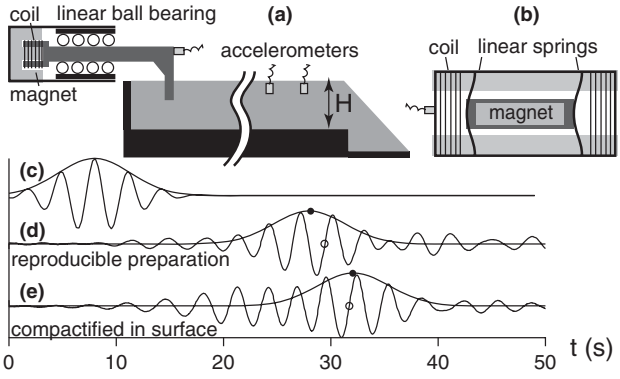

FIG. 1. (a) Experimental setup. Acoustic source of sagittal waves. (b) Acoustic source of transverse waves. (c) Signal of the accelerometer mounted on the source. (d),(e) Transverse wave packets received at $x = 60$ cm from the source, for two preparations of the granular packing (see text). Note the shift of the wave-packet center (●) and of the phase (○).

[Fig. 1(b)]. The channel is filled of glass beads ($E = 70$ GPa, $d = 150 \pm 25$ μm) over the height $H = 20$ cm. For such an aspect ratio, with smooth boundaries, the Janssen effect is negligible [16] so that the pressure is expected to vary linearly in depth. The acoustic isolation is insured by 20-cm-thick boundaries. The experiment is also designed to prevent another problem. As the sample presents random heterogeneities, the acoustic signal is composed by an effective medium response and a coda related to speckle effect [17]. Their relative amplitude is controlled by the number of grains in contact with the transducer. We have chosen to work with accelerometers of diameter $D = 13$ mm, which allow one to measure the three components of the acceleration in the bulk of the sample. Around 3×10^4 grains are in contact with the transducer and the measured amplitude of the coda tail is around 5% of the coherent signal. By comparison, other techniques like a laser vibrometer would only probe the rough surface of the packing and, due to the small size of the spot (5 mm), would only average over ~400 grains, yielding a coda and a coherent signal of the same order of magnitude. We have also checked that the propagation is not affected by the presence of other accelerometers between the source and the receiver. Besides, the transducer size D should be at least a fraction of the wavelength λ, which imposes to work at rather low frequencies $f <$ 1 kHz. In summary, the experiment has to be analyzed keeping in mind the hierarchy of length scales: $d \ll D < \lambda < H$.

The typical vibration amplitude we use is ~10 nm, although the propagation properties remain the same up to ~100 nm, i.e., a strain of 10^{-6}. Above, new peaks appear in the signal and period doubling is observed in the coda, and nonlinear coupling between modes may then happen. Therefore, here we dwell far from the nonlinear propagation conditions (soliton waves) as evidenced ear-

lier in nonlinear Hertz chains [18]. The preparation of the sample is amongst the most difficult parts of the experiment. Prior to each measurement, we systematically sweep a thin blade longitudinally and transversely through the packing in order to remove any memory effect due to the granular initial filling or the subsequent accelerometers manipulation. The extra sand above the level of the channel is then gently removed, leaving a flat surface. Figure 1 compares a typical signal obtained with this procedure [panel (d)] to that obtained when pouring the grains and flattening the surface by tapping with a hammer on a plaster float [panel (e)]. In the first case, the phase and the travel time of the wave packet is reproducible. By contrast, the apparent phase velocity and group velocity can vary up to 25% from one sample to the other, although they are macroscopically identical. This nonuniversality is the first important conclusion of this Letter: the packing elastic properties depend on the preparation protocol. Figure 2 shows the positions of the center of the wave packet and of an isophase event as a function of time. For this, we prepared ~20 realizations of the packing. For each, the signals of four accelerometers placed at different positions are acquired and fitted by a Gaussian wave packet. The propagation of a coherent mode—and not speckle—is clearly evidenced by the linear relationship between space and time and by the reproducibility over independent microscopic realizations. The slopes of the relations give the group and the phase velocities v_g and v_ϕ, respectively. Looking now in depth, the vibration amplitude is observed to decrease over a distance Δ of the order of a half wavelength [Fig. 3(b)]. The sagittal waves are elliptically polarized, with their principal axis in the vertical direction and along the direction of propagation. Figure 3 shows that the shape of the first mode is in fair agreement with the prediction of our model [10], which confirms that the first mode has been successfully isolated, as desired.

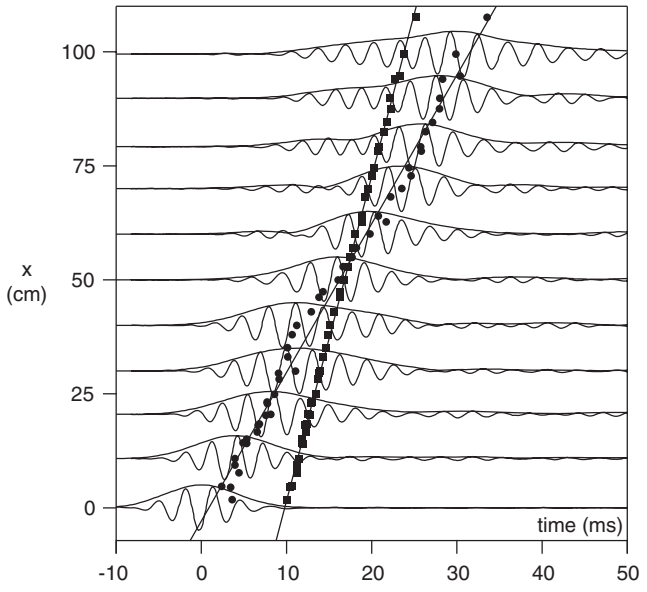

FIG. 2. Space-time diagram showing the wave-packet propagation. Starting from the raw signals received at different positions, the wave packet is roughly localized by computing the signal envelope. Then, a local fit by a Gaussian wave packet allows one to determine the center of the wave packet (●) and its phase with respect to the source (the symbols ■ show the space-time coordinates of an isophase event). The best fit (thin lines) allows one to extract the group and phase velocities.

We have measured v_g and v_ϕ, as well as their statistical uncertainty, every 3 Hz, up to 750 Hz for sagittal waves and up to 550 Hz for transverse waves. These values are used to reconstruct accurately a single dispersion relation $f(\lambda^{-1})$ (Fig. 4) that simultaneously fits the group and phase velocities in the least square sense. As expected, the propagation is dispersive since v_g and v_ϕ are different. This can be related to the two wave-guide effects previously mentioned. The propagation suddenly stops below 180 ± 20 Hz, an effect due to the finite depth and width. For sagittal waves, we observed that this cutoff frequency is associated to a sharp resonance at 192 Hz, with a Q factor of 70. The group velocity is expected to vanish at this frequency and the phase velocity to diverge, which explains the increase of the ratio v_g/v_ϕ with f. Below 300 Hz, we have observed that the wave packets were very distorted and it was not possible to determine v_g and v_ϕ. At high frequency, an asymptotic behavior controlled by the pressure induced wave guide is reached in the limit of wavelengths λ small in front of the channel transverse dimensions (H and W). The ratio v_g/v_ϕ tends to a constant equal to 0.82 ± 0.04 for the preparation described above. As v_g is the slope of the dispersion relation, v_g/v_ϕ is the scaling exponent between f and λ^{-1}. The measured value is very close to that expected if $\mathcal{A}$ does not vanish at the surface $(5/6)$. Thus, our experimental results fully confirm the Hertzian picture down to $\lambda \sim 250d$ and does not show any evidence of anomalous exponent $(2/3)$ when $p \to 0$, which would be associated to a critical behavior at the jamming point [2,13]. It would be interesting to pursue

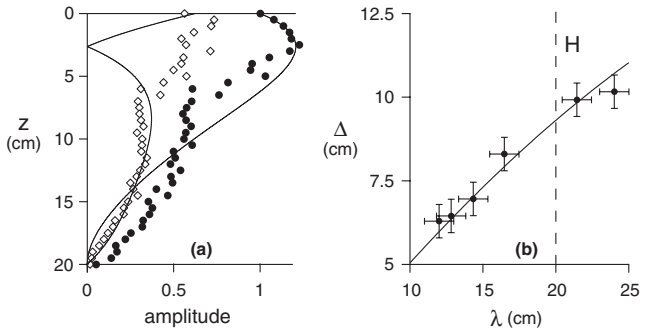

FIG. 3. First sagittal mode. (a) Amplitude of the vertical (●) and horizontal (○) displacement as a function of depth, for $f = 315$ Hz ($\lambda \simeq 21.5$ cm). (b) LengthΔ over which the vibration decays as a function of the wavelength λ.

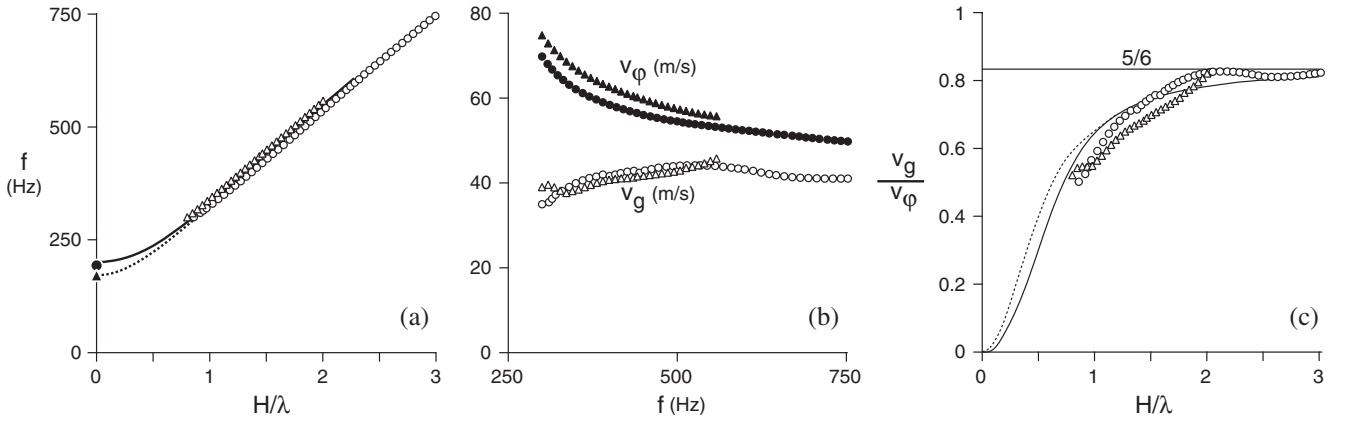

FIG. 4. (a) Dispersion relation of sagittal (○) and longitudinal waves (△): frequency f as a function of the rescaled wave number H/λ. The cutoff frequencies (● and ▲) below which no propagation is observed are measured independently. (b) Corresponding group v_g (open symbols) and phase v_ϕ (solid symbols) velocities. (c) Ratio of the group and phase velocities v_g/v_ϕ as a function of H/λ. In the three graphs, only one-fifth of the measured points are shown. The predictions of the model, including the finite width and depth, are shown as solid (sagittal) and dotted (transverse) lines.

this technique to lower the probing wavelengths in order to push the limits to weaker confining pressures. But to this purpose, the limitations due to finite probe size, preparation sensitivity, and speckle noise have to be overcome.

Globally, one can compare the experimental data to the prediction of the model, assuming that $\mathcal{A}$ does not vanish at the surface and remains nearly constant at the scale λ and taking into account the finite width and depth (lines in Fig. 4). The agreement is excellent (within 5%). The dispersion relations of transverse and sagittal modes turn out to be nearly equal (Fig. 4). This striking behavior is one of the robust outputs of our model [10]. For ratios $\mathcal{B}/\mathcal{A} = O(1)$, the difference would only be of 10% and would be almost indistinguishable when, say, $\mathcal{A} < 0.2\mathcal{B}$. The physical reason is that the restoring force for both modes is the shear elasticity (parameter $\mathcal{A}$). In the limit $\lambda \ll H$, the dispersion relation of the first modes takes the following form:

$$f = \alpha(E/\rho)^{1/3} g^{1/6} \lambda_\infty^{-5/6}, \quad \text{with} \quad \alpha \simeq 0.77 \mathcal{A}^{1/2} \mathcal{B}^{-1/6}. \tag{3}$$

The best fit gives $f\lambda_\infty^{5/6} \simeq 77 \pm 1\ \mathrm{m}^{5/6}\mathrm{s}^{-1}$, which corresponds to a value of $\mathcal{A}^{1/2}\mathcal{B}^{-1/6} \sim 0.23$. By contrast, the mean-field expectation is 0.40 for frictionless grains and 0.61 for infinite friction. Thus, the measured shear stiffness is 3 to 5 times smaller than predicted by the mean-field theory, as observed in numerical simulations [12]. The soft-mode theory is the only one explaining this mean-field failure. Still, to be consistent with our results, one has to conclude that the packing does not tend to isostaticity at the surface: for frictional packings prepared in a simple way, Z remains significantly larger than Z_{iso} under vanishing pressure.

We thank D. Pradal, D. Renard, T. Darnige, and J. Lanuza for their technical assistance and P. Claudin for his critical reading of the manuscript.

[1] C. S. O'Hern, L. E. Silbert, A. J. Liu, and S. R. Nagel, Phys. Rev. E **68**, 011306 (2003).
[2] M. Wyart, L. E. Silbert, S. R. Nagel, and T. A. Witten, Phys. Rev. E **72**, 051306 (2005).
[3] A. Tanguy, J. P. Wittmer, F. Leonforte, and J.-L. Barrat, Phys. Rev. B **66**, 174205 (2002).
[4] E. Somfai *et al.*, Phys. Rev. E **75**, 020301(R) (2007).
[5] V. Magnanimo *et al.*, Europhys. Lett. **81**, 34 006 (2008).
[6] P. H. Brownell, Science **197**, 479 (1977); Sci. Am. **251**, 94 (1984); P. H. Brownell and R. D. Farley, J. Comp. Physiol. **131**, 23 (1979); **131**, 31 (1979).
[7] G. S. Baker, C. Schmeissner, D. W. Steeple, and R. G. Plum, Geophys. Res. Lett. **26**, 279 (1999).
[8] B. Andreotti, Phys. Rev. Lett. **93**, 238001 (2004).
[9] V. E. Gusev, V. Aleshin, and V. Tournat, Phys. Rev. Lett. **96**, 214301 (2006); X. Jacob *et al.*, Phys. Rev. Lett. **100**, 158003 (2008).
[10] L. Bonneau, B. Andreotti, and E. Clément, Phys. Rev. E **75**, 016602 (2007).
[11] Y. Jiang and M. Liu, Phys. Rev. Lett. **91**, 144301 (2003); **93**, 148001 (2004).
[12] H. A. Makse, N. Gland, D. L. Johnson, and L. M. Schwartz, Phys. Rev. Lett. **83**, 5070 (1999); Phys. Rev. E **70**, 061302 (2004).
[13] K. Shundyak, M. van Hecke, and W. van Saarloos, Phys. Rev. E **75**, 010301(R) (2007).
[14] N. Xu, M. Wyart, A. J. Liu, and S. R. Nagel, Phys. Rev. Lett. **98**, 175502 (2007).
[15] B. Andreotti, L. Bonneau, and E. Clément, Geophys. Res. Lett. **35**, L08306 (2008).
[16] G. Ovarlez, C. Fond, and E. Clément, Phys. Rev. E **67**, 060302(R) (2003).
[17] X. Jia, C. Caroli, and B. Velicky, Phys. Rev. Lett. **82**, 1863 (1999).
[18] S. Job, F. Melo, A. Sokolow, and S. Sen, Phys. Rev. Lett. **94**, 178002 (2005).